Characterization of the ultrafast nonlinear response of new organic compounds

David Hagan, Salimeh Tofighi, Sepehr Benis, Hao-Jung Chang, Ryan O'Donnell, et al.

David J. Hagan, Salimeh Tofighi, Sepehr Benis, Hao-Jung Chang, Ryan M. O'Donnell, Jianmin Shi, Mikhail V. Bondar, Eric W. Van Stryland, "Characterization of the ultrafast nonlinear response of new organic compounds," Proc. SPIE 11277, Organic Photonic Materials and Devices XXII, 112770N (28 February 2020); doi: 10.1117/12.2552364

SPIE.

Event: SPIE OPTO, 2020, San Francisco, California, United States

Characterization of the ultrafast nonlinear response of new organic compounds

David J. Hagan[1], Salimeh Tofighi[1], Sepehr Benis[1], Hao-Jung Chang[1], Ryan M. O'Donnell[2], Jianmin Shi[2], Mikhail V. Bondar[1,3], and Eric W. Van Stryland[1]

[1]CREOL, The College of Optics and Photonics, University of Central Florida, Orlando, Florida 32816, United States

[2]US Army Research Laboratory, Adelphi, Maryland 20783, USA

[3]Institute of Physics NASU, Prospect Nauki, 46, Kyiv-28 03028, Ukraine

ABSTRACT

Here, we present our development of several experimental methods, which, when applied together, can provide a thorough characterization of the nonlinear refraction and absorption properties of materials. We focus mainly on time-resolved methods for studying both transient absorption and refraction that reveal molecular dynamics including excited-state absorption, singlet-triplet transfer, instantaneous electronic nonlinear refraction, and molecular reorientation. In particular, we will describe our recent studies of new materials including organometallic compounds and organic solvents such as Tetrachloroethylene (C_2Cl_4).

Keywords: Ultrafast nonlinear optics, Nonlinear optical materials, Organic compounds, Organic solvents

1. INTRODUCTION

Nonlinear optical (NLO) properties of organic compounds and solvents are of great interest in many fields, including nonlinear fluorescence imaging [1, 2], organic optoelectronics [3, 4], optical data storage [5, 6], and nonlinear optics in liquid-core optical fibers [7-9]. Mechanisms such as nonlinear absorption (NLA) and nonlinear refraction (NLR) are two well-studied properties of organic materials, mainly due to their ability to tailor the optical response through variations in the molecular structure [10-12]. Typically, the main contributions to NLA are two-photon absorption (2PA) and excited state absorption (ESA). For NLR, the instantaneous bound-electronic refraction, dominates for short timescales, while excited state refraction and molecular reorientation are observed on longer time scales. Here, we review our development of several nonlinear spectroscopic techniques. These methods pave the way towards understanding the origin of NLO response of materials and provides insight into relating nonlinearities to their molecular structures. Ultimately, this knowledge allows engineering the transient nonlinear absorptive and refractive properties of solutions of organic dyes and pure solvents.

In nonlinear organic materials, ESA is typically observed in molecules that have excited state absorption cross-sections that are higher than in the ground state. Typically these decay on a picosecond to nanosecond timescales. Adding a heavy metal to the organic molecules can increase spin-orbit coupling that can result in higher triplet quantum yields [13-15]. Since triplet states are long-lived, this can result in nonlinear absorption with lifetimes as long as microseconds. In these organometallic complexes, ESA and singlet-triplet transfer also play an important role in applications such as organic light-emitting diode [16, 17], bioimaging [2, 14], and others [13, 18-21]. The challenge in nonlinear spectroscopic characterization of these molecules is the decoupling of the triplet-triplet cross section (σ_T) from the singlet-triplet quantum yield (ϕ_{ST}). Various methods have been developed for this purpose [22-24]. Some of these techniques rely on comparison with a reference compound. In some cases, there are insufficient reference materials which can result in an accumulation of error. In our group, we use the double pump-probe (DPP) technique to directly measure the triplet population processes of organometallic complexes [25-28].

Similarly, NLR and its associated temporal dynamics are also of great importance in organic NLO applications, particularly in the visible and near-IR spectral regime. In this spectral window, solvents are mainly transparent and lack NLA processes such as 2PA. However, nuclear nonlinearities including molecular reorientation contribute to the NLO response at longer pulse widths, which has led to disagreement in NLR coefficients reported in the literature. Such disagreement is sometimes because single-beam methods such as Z-scan [29] do not distinguish between slower molecular

Organic Photonic Materials and Devices XXII, edited by Christopher E. Tabor, François Kajzar, Toshikuni Kaino, Proc. of SPIE Vol. 11277, 112770N
 · doi: 10.1117/12.2552364

reorientation and instantaneous bound electronic nonlinearities. Our Beam-Deflection (BD) method [30], being time-resolved and allowing for different relative polarization combinations of pump and probe beam, does not suffer from this constraint. This technique allows us to calculate the NLR response function over the temporal range from 10 fs to 1 ns. The knowledge of NLO response function of solvents is essential to obtain refractive parameters of organic compounds dissolved in solvents.

2. EXPERIMENTAL TECHNIQUES

2.1 Z-scan

The Z-scan technique, invented in 1989 [29, 31], is a simple method that has become popular in nonlinear spectroscopy for studying nonlinear refraction and absorption. This method only requires a single beam and measures the temporally-averaged sign and magnitude of both NLA and NLR through the thickness of a sample with interferometric sensitivity. In this method, the sample is translated axially through the focus of a beam, and the energy of the transmitted beam in the far-field is measured. The open aperture (OA) Z-scan, in which the total transmitted energy is collected, directly measures the NLA including instantaneous multiphoton absorption, e.g. 2PA and three-photon absorption (3PA), and slow higher order processes such as ESA. However, in the closed aperture (CA) Z-scan, a partially closed aperture is used to measure the induced nonlinear phase shift. In this case, both NLA and NLR contribute to the detected signal, and by dividing the OA signal we can extract the contribution of the NLR to the measurements. This technique has been expanded to several forms such as two-color Z-scan [32], eclipsing Z-scan [33], Z-scan for thick samples [34], and more recently dual-arm Z-scan [35, 36]. In particular, the dual-arm Z-scan has several advantages such as better signal-to-noise ratio and enhanced sensitivity for measuring small NLR of organic molecules (in solution form) [36] and thin-films [35]. However, the Z-scan technique does not measure the time dynamics of the NLO parameters, so it provides only a limited picture of the physics of the NLO response.

2.2 Pump-probe methods

Although the Z-scan technique is proven to be versatile in measuring material nonlinearities, it does not give information on their temporal response. However, pump-probe methods that utilize two pulses with variable relative delay, can be used to time-resolve the NLO response. For the study of NLA, a strong, monochromatic pump pulse passes through the sample, inducing absorption that is experienced by a weak probe pulse that passes through the same volume of the sample with a certain delay after the pump pulse. If the NLA response is instantaneous, e.g. 2PA or 3PA, the resulting probe transmission versus delay reveals the cross correlation between the pump and probe. However, if the pump generates long-lived excitations in the material, the absorption spectrum of the material is changed. This changes the probe transmittance and as we vary the probe delay, we can observe the relaxation of these excitations with a time resolution limited by the cross-correlation of the pump and probe. The probe can be a narrowband pulse to measure the NLA at that wavelength, but as we shall show there are some variations of the method that allow broadband spectral characterization of NLA, as well as temporal dynamics of NLR.

2.2.1 Transient absorption spectroscopy

The spectral dependence of the NLA can be reconstructed by several different narrowband pulses at different wavelengths or straightforwardly measured by a broadband probe pulse. A white-light continuum (WLC) pulse can be used as the probe and the induced change in the transmission of probe is measured by a spectrometer with a CCD or photodiode array [37, 38] as shown in **Figure 1**. This WLC pulse is generated by focusing a strong pump beam into a thick transparent medium such as a sapphire plate or a thick cuvette of pure water [37].

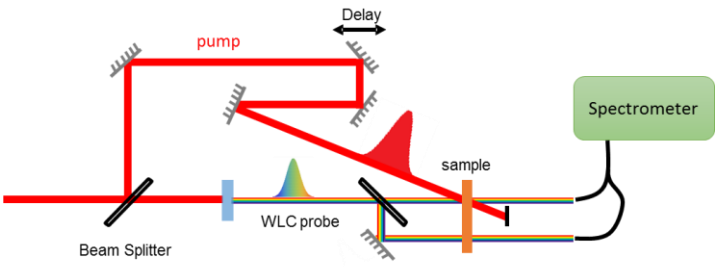

Figure 1. Transient absorption spectroscopy experimental setup.

2.2.2 Double-pump and probe

For molecules with accessible triplet states, alongside the amount of population change from singlet to triplet state that is characterized by the triplet quantum yield, ϕ_{ST}, the change in the triplet transient absorption is also dependent on the triplet cross section, σ_T. As a result, the nonlinear transient absorption seen in a conventional pump-probe experiment is a combined effect of both of these parameters as it can only quantify $\phi_{ST} \times \sigma_T$. For decoupling ϕ_{ST} and σ_T values from each other Swatton et al. [39] suggested adding another pump to the conventional pump-probe technique. In the case of double pump-probe method, the first pump populates the triplet state through the intersystem crossing of population absorbed by the singlet excited state [25]. The resultant change in absorption will depend on both the singlet and triplet lifetimes. By adding a second pump, the probe experiences a system with a different population distribution where the triplet states have also been populated. By measuring the induced change in absorption by both pumps and modeling the system with an appropriate electronic model, we can decouple ϕ_{ST} and σ_T values. Figure 2 shows the schematics of the double-pump probe experiment.

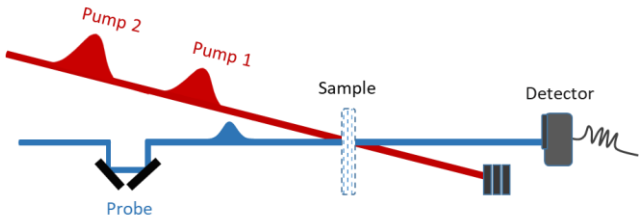

Figure 2. Double pump-probe experimental setup

2.2.3 Beam-deflection

Various experimental techniques are devoted to measuring the NLR of NLO materials. For example, Z-scan [29] measures the magnitude and sign of the NLR and NLA, however, it lacks information on the transient NLO response. Additionally, optical Kerr experiments (OKE) [40] give the temporal response of the induced birefringence, but it does not directly measure the nonlinear refraction nor the NLA. The BD technique [30, 41-43] allows simultaneous characterization of the sign, magnitude, and ultrafast dynamics of both NLA and NLR in solids [44-46], liquids [41-43, 47], and gases [48, 49]. Particularly, the ability to control the wavelength and polarization of each beam enables the possibility to characterize the nondegenerate NLR and NLA and the relative polarization anisotropy of the NLO response. These advantages help to obtain detailed information on the physical origin of the mechanism behind the optical nonlinearities and to construct the spectral dependence of the NLO response. The knowledge of the noninstantaneous NLR of solvents and their NLO response function has gained attention in several fields such as generation of hybrid soliton dynamics and dispersive waves in liquid-core optical fibers [9, 50, 51], and also in engineering the transients of NLR of solutions making them possible candidate materials for organic all-optical modulation applications [43] and efficient continuum generation [4, 7, 8, 50-53].

The principle of the BD method, shown in Figure 3(a), is similar to transient absorption spectroscopy with some modifications for measuring transient NLR. This method directly measures the nonlinear phase shift imposed on the probe beam induced by a strong pump pulse. In BD, a temporally delayed probe with spatial dimensions ~ 3-5 × smaller than that of the pump is focused in the wings of the pump beam where the index gradient is maximized. The induced index gradient deflects the probe beam as measured using a position sensitive quad-segmented detector in the far-field as shown in Figure 3(b, c). The normalized deflection signal, $\Delta E/E$, is the ratio between the difference of energy on the two sides of the detector, ΔE, to the total transmitted signal, E. In the limit of small NLA, this ratio is directly proportional to the induced nonlinear phase shift on the probe beam, hence NLR. Similarly, the normalized change in the total transmission signal, $\Delta T/T$ can be used to directly characterize the NLA. In pure solvents, there is no NLA in the visible or near-IR. However, for organic compounds dissolved in solvents, $\Delta E/E$ and $\Delta T/T$, which obtained from BD can simultaneously characterize both NLR and NLA.

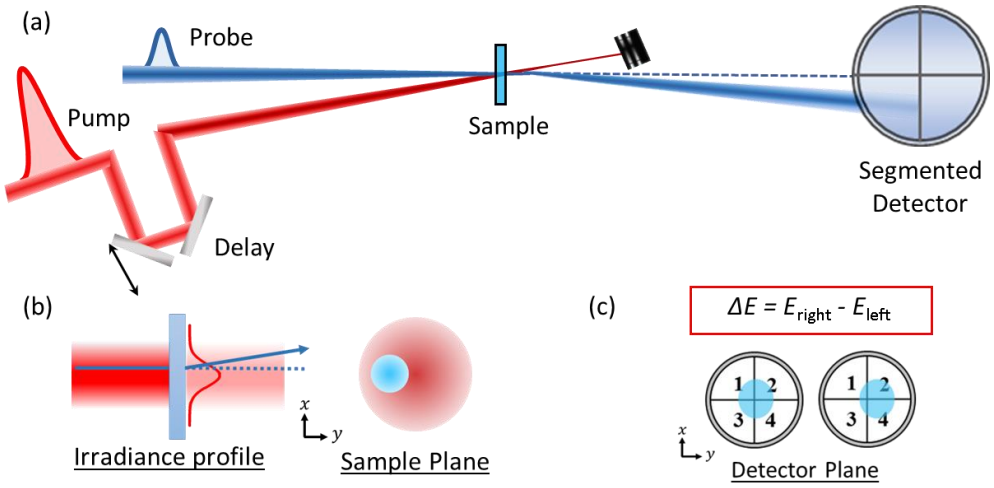

Figure 3. (a) Experimental schematics of BD setup; (b) spatial irradiance distribution of the pump beam overlapping with the probe beam with a smaller size (left) from top and (right) at the sample plane; (c) probe beam on the segmented detector with and without deflection.

3. CHARACTERIZATION OF ORGANIC COMPOUNDS AND SOLVENTS

3.1 Transient absorption spectroscopy of gold-dithiolenes

We performed transient absorption spectroscopy measurements on a series of metal dithiolene compounds. These compounds have shown a broad ESA spectrum and photostability that can be used as near-IR laser dyes [54]. As a candidate material, we present our measurements on TBA[Au^{III}(SCCPhOMe)4] (Au-OMe), shown in Figure 4(a), which is dissolved in acetonitrile and filled in a 1 mm thick quartz flow cell. Flowing of the solution is to reduce the effect of photochemical decomposition in our measurements. In this experiment, a 1 kHz Ti:Sapphire regenerative amplifier (Legend Duo+, Coherent, Inc.) with output wavelength, $\lambda = 800\ nm$ is used. The second-harmonic of the output at 400 nm is used as the pump pulse. Part of the 800 nm beam is focused into a 1 cm thick quartz cell filled with water to produce a WLC probe pulse (~430 nm to 730 nm).

We performed pump-probe measurements on Au-OMe compound, shown in Figure 4(a), to characterize the ESA cross-section. We spectrally filtered the WLC probe pulse to generate narrowband (~ 10 nm) pulses at 480 nm, 550 nm, and 650 nm. Experimental data are shown in Figure 4 (b-d), respectively. The energy of the transmitted probe is collected by a silicon photodiode with a lock-in amplifier to improve the signal-to-noise ratio. As shown in Figure 4 (b-d), we observe ESA at longer delays with different lifetimes for each wavelength.

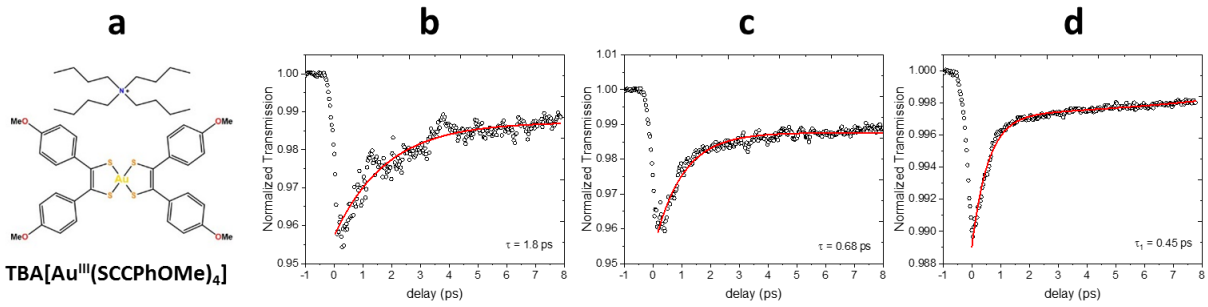

Figure 4. (a) Molecule structure and pump-probe of Au-OMe with probe wavelength at (b) 480 nm, (c) 550 nm, and (d) 650 nm. The ESA lifetime for each wavelength is presented in the corresponding figure.

3.2 Study of triplet quantum yield in Iridium complexes

We also studied several organonmetallic iridium complexes, provided by ARL [26]. In Figure 5 some of these compounds are shown. We performed different linear spectroscopic measurements including photoluminescence emission and decay measurements prior to performing any nonlinear measurements [55]. The photoluminescence decay measurements, indicating the presence of both fluorescence and phosphorescence, prove that these compounds have both singlet and triplet excited states. Therefore, we use our DPP technique to efficiently decouple the ϕ_{ST} and σ_T values.

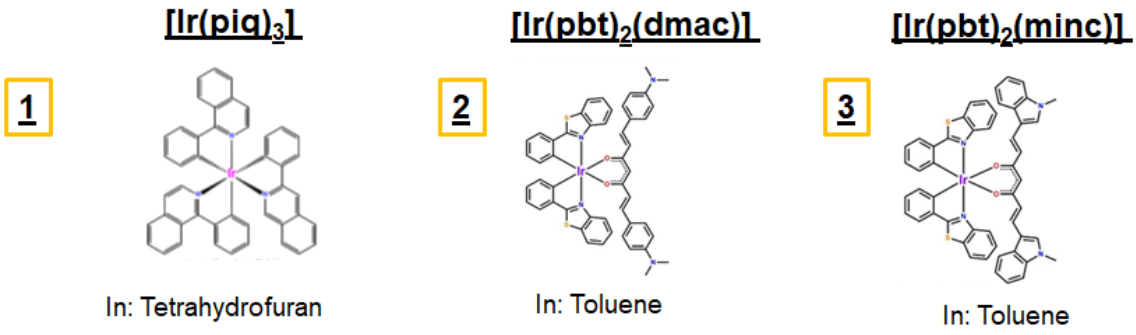

Figure 5. Chemical structure of three organometallic complexes and the solvent used for each measurement.

We used the second harmonic of a Nd:YAG laser system at 532nm (PL-2143, EKSPLA Co.) with a pulse duration of ~29 picoseconds and 10 Hz repetition rate to perform degenerate DPP measurements. We also used a femtosecond laser system to perform similar measurements to resolve the fast dynamics of these compounds. For the femtosecond measurements, we used a thick BBO crystal to double the 800 nm output of a Ti:sapphire laser system (Legend Duo+, Coherent, Inc.) with 40 fs pulse duration and 1 kHz repetition rate. A portion of the 800 nm output beam was focused on a 1 cm thick cuvette filled with water to generate WLC and filtered by a 550 nm bandpass filter as a probe beam.

For the majority of the organometallic samples, a conventional five-level electronic model, Figure 6(a), with singlet ligand centered (LC) and triplet metal-to-ligand charge transfer (MLCT) excited state was used to fit the data for various energies [26]. For some of the compounds, such as sample (2), we could fit the data for one set of excitation energies but we could not fit the data with the same fitting parameters for another set of energies using the five level model. This shows the need for a modified electronic model to describe the NLO behavior of these molecules. This led to the development of a 6-level model, shown in Figure 6(b). This model includes a short-lived intermediate MLCT singlet state, which allows us to fit the data for different sets of excitation energies.

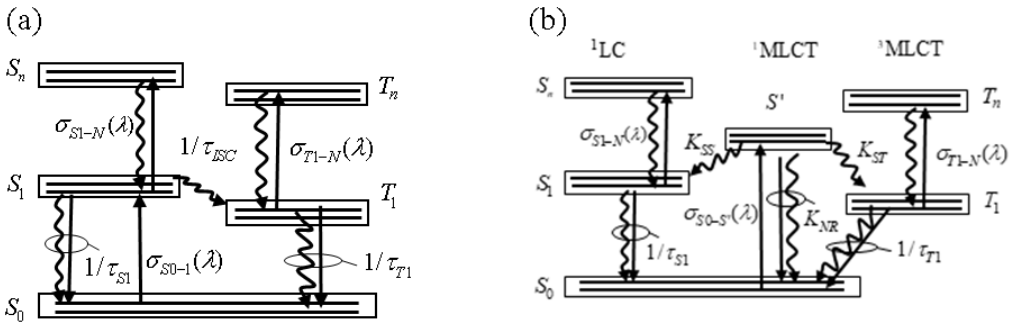

Figure 6. (a) 5-level and (b) 6-level electronic model used for the fitting

The following sets of rate equations were used for fitting the data for six level electronic system. We assume that all lifetimes of the higher excited electronic states (S_n and T_n) are short enough that their populations are negligible, and the excitation intensities are not depleted due to additional ESA processes at the excitation wavelength. The details of this model are also presented in [26].

$$\frac{\partial N_{S0}}{\partial t} = -N_{S0}\frac{\sigma_{S0-S'}(\lambda_e)(I_{e1}+I_{e2})}{\hbar\omega_e} + N_{S'}K_{NR} + \frac{N_{S1}}{\tau_{S1}} + \frac{N_{T1}}{\tau_{T1}},$$

$$\frac{\partial N_{S'}}{\partial t} = N_{S0}\frac{\sigma_{S0-S'}(\lambda_e)(I_{e1}+I_{e2})}{\hbar\omega_e} - N_{S'}(K_{SS}+K_{NR}+K_{ST}),$$

$$\frac{\partial N_{S1}}{\partial t} = N_{S'}K_{SS} - \frac{N_{S1}}{\tau_{S1}},$$

$$\frac{\partial N_{T1}}{\partial t} = N_{S'}K_{ST} - \frac{N_{T1}}{\tau_{T1}}, \qquad (1)$$

$$\frac{\partial I_{e1(2)}}{\partial t} = -N_{S0}\sigma_{S0-S'}(\lambda_e)I_{e1(2)} - N_{S1}\sigma_{S1-N}(\lambda_e)I_{e1(2)} - N_{T1}\sigma_{T1-N}(\lambda_e)I_{e1(2)},$$

$$\frac{\partial I_p}{\partial t} = -N_{S0}\sigma_{S0-S'}(\lambda_p)I_p - N_{S1}\sigma_{S1-N}(\lambda_p)I_p - N_{T1}\sigma_{T1-N}(\lambda_p)I_p,$$

$$\Phi_{ST} = \frac{K_{ST}}{K_{SS}+K_{NR}+K_{ST}},$$

Below, we show the data and fit for the picosecond DPP measurements on sample 2. In [26-28] we also reported the results for several other organometallic compounds. In these measurements, our results indicate that the triplet quantum yield is below unity for all the compounds.

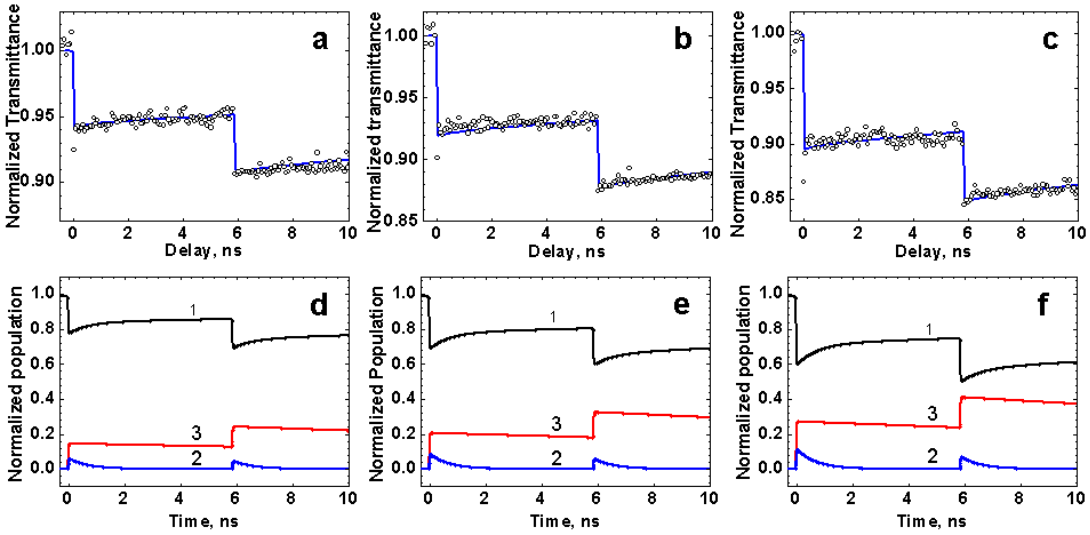

Figure 7. (a-c) Picosecond transient absorption DPP curves (circles) and corresponding fits (solid lines) for a 0.37 mM solution of sample #2 in Toluene with pump and probe wavelengths at 532 nm for energies of the first and second pump of (a) $E_{e1} = 9.3\ \mu J$, $E_{e2} = 11\mu J$, (b) $E_{e1} = 14\ \mu J$, $E_{e2} = 15\ \mu J$, and (c) $E_{e1} = 20\ \mu J$, $E_{e2} = 21\ \mu J$. (d-f) Calculated kinetic changes in the populations of S0 (black), S1 (blue), and T1 (red) electronic states from the fittings in (a-c), respectively.

3.3 Characterization of NLR in organic solvents

Here, we briefly present the experimental conditions and summarize the work that has been done in our group on characterizing the NLO response function of solvents. We also present our recent measurements on C_2Cl_4 (Tetrachloroethylene or TCE) and our predictions on its effective NLR over a range of pulsewidths. Our BD measurements were all performed using femtosecond lasers with 1 kHz repetition rates, and pulsewidth of 40 fs (Coherent Legend Elite Due HE +) or 150 fs (Clark-MXR). The pump beam is centered at 800 nm (for 40 fs laser source) and 775 nm (for 150 fs laser source). The probe beam is from a white-light continuum generated by pumping a transparent medium such as a cuvette of pure water, or a thick sapphire plate and filtered with a narrowband (~ 10 nm) filter at 700 nm.

Several mechanisms contribute to the NLO response function of solvents. The third-order bound-electronic response of isotropic liquids, $n_{2,el}$, is the only mechanism that happens instantaneously, and it is directly proportional to the second

hyperpolarizability, γ. Additionally, several nuclear NLO effects with slower response times contribute to the NLO response function. These effects are due to the optically induced dipole moment that results in a torque imposed on the molecules aligning them towards the field direction as well as a collisional response [40, 48, 49]. Thus, the change in the refractive index depends upon the polarizability anisotropy of the molecule as discussed in [43]. The overall induced change in NLR can be explained via

$$\Delta n = n_{2,el} I(t) + \int_{-\infty}^{\infty} R(t-t') I(t') dt', \tag{2}$$

where $I(t)$ is the irradiance, $n_{2,el}$ is the bound electronic NLR coefficient, and $R(t)$ is the nuclear NLO response function. For the pulsewidths used in our studies, $R(t)$ is a superposition of three linearly independent contributions namely diffusive reorientation, which produces a torque on the molecule, molecular libration, where the torque results in a rocking motion, and collision-induced changes in the molecular polarizability. For very short pulses, vibrational modes can also be excited through the stimulated Raman effect that can also be considered in the response function [43]. Here, we ignore this effect as a narrowband femtosecond pulse is used, thus the pulsewidth is much longer than the typical vibrational period. The symmetry of bound-electronic and collision-induced NLR follows the isotropic symmetry of the liquid; however, the laser pulse induces a relative polarization anisotropy in the liquid resulting in a different symmetry for molecular reorientation and libration than that of bound electronic nonlinearities. By resolving the relative polarization-dependence of the BD signal and measuring the transients of the NLR, we can accurately characterize the sign, magnitude, and time-dynamics of each process and predict the NLO response function of the solvent. The details of the temporal- and polarization-dependence of each mechanism and its formalism are presented in [41, 42], where we fully characterized the NLO response function of liquid CS_2. For CS_2, we also performed Z-scan measurements for various pulsewidths and compared the values of $n_{2,eff}$, defined by $\Delta n = n_{2,eff} I$, for linear polarization with the predicted response function extracted from BD measurements. The comparison of the results is shown in Figure 8.

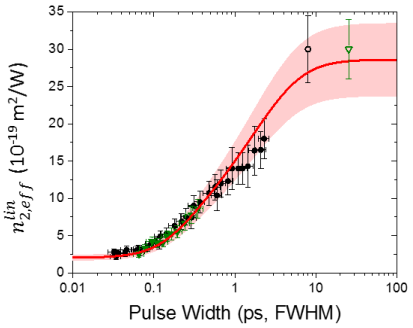

Figure 8. Comparison of Z-scan measurements (data) and calculation of $\boldsymbol{n_{2,eff}}$ (red curve), of CS2 versus pulsewidth. The shaded region is the errors in the response function [41, 42].

There have been orders-of-magnitude discrepancies in reported values of NLR of solvents in the literature, mainly due to the dependence of the nonlinearly induced changes in refractive index on the pulsewidth [43]. Our BD method has successfully addressed this problem by predicting the pulsewidth dependence of the NLO response function. To accurately compare the values measured by BD with other techniques, we define the effective NLR, $n_{2,eff}$, as

$$n_{2,eff} = n_{2,el} + \frac{\int I(t) \int R(t-t') I(t') dt' \, dt}{\int I^2(t) dt}, \tag{3}$$

In the limit of short pulses the $n_{2,el}$ is predominant; however, $n_{2,eff}$ monotonically increases with pulsewidth due to the contribution of noninstantaneous effects. In the long pulse limit, $n_{2,eff}$ is given by sum of each component's magnitude. We recently characterized the NLO response function of 24 common solvents [43], including families of benzene derivatives, haloalkanes, ketones, nitriles, formamides, esters, ethers, alkanes, alcohols, heavy water, pure water, and CS_2. We find that nonconjugated molecules exhibit negligible reorientational response because of their small polarizability anisotropy, thus the effective NLR is almost independent of the pulsewidth. Below we show the prediction of magnitude of the effective NLR with pulsewidth for different solvents. The detail of the measurements including the NLO response function of each solvent is presented in [41-43].

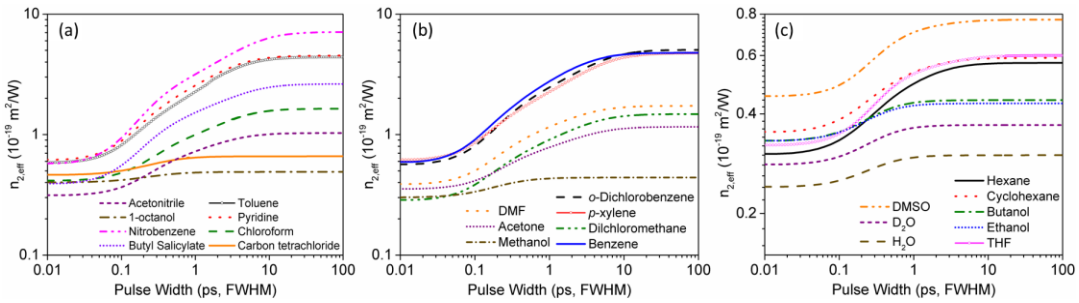

Figure 9. Predictions of pulsewidth dependent $n_{2,eff}$ of various solvents from [43].

We recently performed BD measurements on C_2Cl_4, which is presented in Figure 10(a). TCE has potential applications in noninstantaneous hybrid solitons [9, 50, 56], supercontinuum generation [7, 8], and harmonic generation [51] in meters long liquid core fibers. In particular, carbon chlorides such as CCl_4 (carbon tetrachloride or CTC) and TCE are extensively used due to their small loss, their superior transmission from visible to mid-IR [53], and higher refractive index contrast with cladding compared to other solvents. Note that CTC is a highly symmetric molecule with zero polarizability anisotropy, hence the NLR lacks any noninstantaneous component due to the absence of molecular reorientation [43]. However, TCE exhibits a very slow decay (> 6 ps) due to the highly anisotropic nature of its polarizability. There are no quantitatively accurate models for the NLO response of TCE in the literature. Our BD technique allows us to extract the sign, magnitude, and dynamics of each mechanism that contributes to NLO response function, as shown in Figure 10(b).

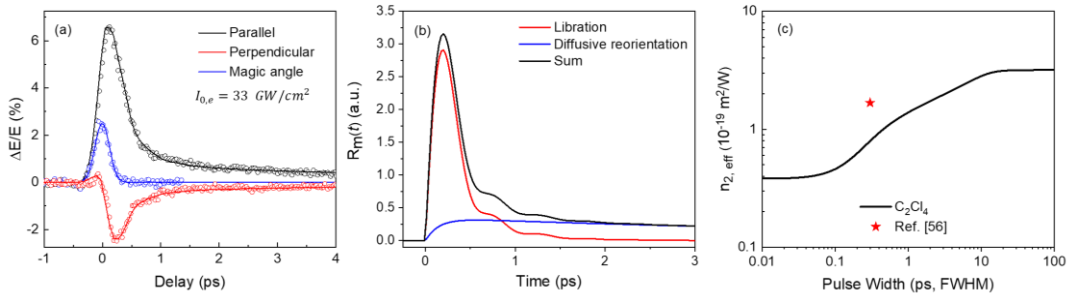

Figure 10. (a) BD measurements (circles) on TCE with fits (lines) for parallel (black), perpendicular (red), and magic angle (blue) relative polarizations of pump and probe, (b) libration (red), diffusive reorientation (blue), and total noninstantaneous components of the NLO response function (c) predicted values of $\boldsymbol{n_{2,eff}}$ for pulsewdiths ranging from 10 fs to 100 ps.

We fit the experiment with our theory developed in [30, 41]. The measurements are conducted at three polarization angles of the probe, with respect to the pump. The blue data and fit (magic angle) isolates NLR with isotropic symmetry, Δn_{iso}, and directly characterizes the sign, magnitude, and time dynamics of the bound-electronic and collision-induced changes in the refractive index, where $\Delta n_{magic} = 5/9\Delta n_{iso}$. When the two beams are co-polarized (parallel), the signal is sum of both isotropic and reorientational effects, Δn_{re}, described via $\Delta n_{parallel} = \Delta n_{iso} + \Delta n_{re}$. However, in the cross-polarized (perpendicular) signal, each mechanism contributes with a scaling, which can be formulated as $\Delta n_{parallel} = 1/3\Delta n_{iso} - 1/2\Delta n_{re}$. The combination of these three cases fully characterizes the magnitude and time-dependence of all the mechanisms. We summarized these parameters for TCE in Table 1.

Table 1. Fit parameters of NLO response of TCE (Tetrachloroethylene)

Mechanism	$n_{2,m}$ [(a)]	Rise time $\tau_{r,m}\ (fs)$	Fall time $\tau_{f,m}\ (fs)$	Symmetry
Electronic	0.38	Instantaneous		iso
Collision	Negligible	–	–	iso
Libration	1	(b)	650	re
Diffusive	1.8	150	6500	re

(a) $n_{2,m}$ are given in units of $10^{-19}\ m^2/W$.
(b) $\omega_0 = 4\ \text{ps}^{-1}$ and $\sigma = 6.5\ \text{ps}^{-1}$

Note that the magic angle data is fit by the cross-correlation of pump and probe pulses, indicating that the instantaneous NLR, i.e. bound electronic nonlinearities, is the only mechanism in this solvent. This means that either the collision-induced changes in the refractive index are negligible or cannot be resolved by our pulsewidth. Finally, the diffusive and librational components are fit using parallel and perpendicular signals. The effective NLR, $n_{2,eff}$, for TCE is also predicted in Figure 10(c).

4. CONCLUSIONS

We presented our experimental capabilities in characterizing the NLO parameters of organic compounds and solvents. We performed a comprehensive investigation of the nonlinear optical properties of organometallic complexes utilizing our transient absorption spectroscopy and double-pump and probe. The transient absorption spectroscopy allows us to investigate the broad ESA spectrum of some of the organometallic complexes such as gold-dithiolenes. Additionally, in organometallic iridium complexes, we used DPP spectroscopic technique using both femtosecond and picosecond lasers to decouple the triplet cross-section from the singlet-triplet quantum yield. A modified electronic model is proposed to describe the NLO behavior of these molecules. Similarly, we presented capabilities of our BD method, fully characterizing the temporal- and polarization-dependence of the third-order NLR of solvents. With this method we are able to measure the NLO response function and predict the $n_{2,eff}$ versus pulsewidth of several solvents from various families; establishing a quantitative reference for those using solvents in NLO applications.

ACKNOWLEDGMENTS

We thank the Army Research Laboratory (W911NF-15-2-0090) and the National Science Foundation (DMR-1609895) for support. MVB wishes to thank the National Academy of Sciences of Ukraine (grants B-180 and VC/188).

REFERENCES

[1] T. S.-M. Tang, H.-W. Liu, and K. K.-W. Lo, "Monochromophoric iridium (iii) pyridyl–tetrazine complexes as a unique design strategy for bioorthogonal probes with luminogenic behavior," Chemical Communications, 53(23), 3299-3302 (2017).

[2] C. Huang, G. Ran, Y. Zhao *et al.*, "Synthesis and application of a water-soluble phosphorescent iridium complex as turn-on sensing material for human serum albumin," Dalton Transactions, 47(7), 2330-2336 (2018).

[3] R. U. Khan, O. P. Kwon, A. Tapponnier *et al.*, "Supramolecular ordered organic thin films for nonlinear optical and optoelectronic applications," Advanced Functional Materials, 16(2), 180-188 (2006).

[4] V. Agranovich, Y. N. Gartstein, and M. Litinskaya, "Hybrid resonant organic–inorganic nanostructures for optoelectronic applications," Chemical reviews, 111(9), 5179-5214 (2011).

[5] B. L. Feringa, W. F. Jager, and B. de Lange, "Organic materials for reversible optical data storage," Tetrahedron, 49(37), 8267-8310 (1993).

[6] H. S. Nalwa, and S. Miyata, [Nonlinear optics of organic molecules and polymers] CRC press, (1996).

[7] M. Chemnitz, C. Gaida, M. Gebhardt *et al.*, "Carbon chloride-core fibers for soliton mediated supercontinuum generation," Optics express, 26(3), 3221-3235 (2018).

[8] R. Kasztelanic, A. Anuszkiewicz, G. Stepniewski *et al.*, "All-normal dispersion supercontinuum generation in photonic crystal fibers with large hollow cores infiltrated with toluene," Optical Materials Express, 8(11), 3568-3582 (2018).

[9] S. V. Palacio, and R. A. Herrera, "Dispersive wave and four-wave mixing generation in noninstantaneous nonlinear fiber solitons," Applied optics, 58(10), 2736-2744 (2019).

[10] D. R. Kanis, M. A. Ratner, and T. J. Marks, “Design and construction of molecular assemblies with large second-order optical nonlinearities. Quantum chemical aspects,” Chemical Reviews, 94(1), 195-242 (1994).
[11] S. R. Marder, J. E. Sohn, and G. D. Stucky, [Materials for nonlinear optics chemical perspectives] American Chemical Society Washington DC, (1991).
[12] D. J. Williams, and P. Prasad, [Introduction to nonlinear optical effects in molecules and polymers] Wiley New York, (1990).
[13] D. Liu, H. Ren, L. Deng *et al.*, “Synthesis and electrophosphorescence of iridium complexes containing benzothiazole-based ligands,” ACS applied materials & interfaces, 5(11), 4937-4944 (2013).
[14] K.-C. Tang, K. L. Liu, and I.-C. Chen, “Rapid intersystem crossing in highly phosphorescent iridium complexes,” Chemical physics letters, 386(4-6), 437-441 (2004).
[15] S. Lamansky, P. Djurovich, D. Murphy *et al.*, “Synthesis and characterization of phosphorescent cyclometalated iridium complexes,” Inorganic Chemistry, 40(7), 1704-1711 (2001).
[16] S. Lamansky, P. I. Djurovich, F. Abdel-Razzaq *et al.*, “Cyclometalated Ir complexes in polymer organic light-emitting devices,” Journal of applied physics, 92(3), 1570-1575 (2002).
[17] L. A. Oro, and C. Claver, [Iridium complexes in organic synthesis] John Wiley & Sons, (2008).
[18] M.-L. Ho, M.-H. Lin, Y.-T. Chen *et al.*, “Iridium (III) complexes in discs for two-photon excitation applications,” Chemical Physics Letters, 509(4-6), 162-168 (2011).
[19] L. Tabrizi, and H. Chiniforoshan, “New cyclometalated Ir (III) complexes with NCN pincer and meso-phenylcyanamide BODIPY ligands as efficient photodynamic therapy agents,” RSC advances, 7(54), 34160-34169 (2017).
[20] Z. Song, R. Liu, Y. Li *et al.*, “AIE-active Ir (III) complexes with tunable emissions, mechanoluminescence and their application for data security protection,” Journal of Materials Chemistry C, 4(13), 2553-2559 (2016).
[21] I. Davydenko, S. Benis, S. B. Shiring *et al.*, “Effects of meso-M (PPh 3) 2 Cl (M= Pd, Ni) substituents on the linear and third-order nonlinear optical properties of chalcogenopyrylium-terminated heptamethines in solution and solid states,” Journal of Materials Chemistry C, 6(14), 3613-3620 (2018).
[22] G. A. Crosby, and J. N. Demas, “Quantum efficiencies of transition-metal complexes. I. dd luminescence,” Journal of the American Chemical Society, 92(25), 7262-7270 (1970).
[23] G. Crosby, and J. Demas, “Quantum efficiencies on transition metal complexes. II. Charge-transfer luminescence,” Journal of the American Chemical Society, 93(12), 2841-2847 (1971).
[24] A. Endo, K. Suzuki, T. Yoshihara *et al.*, “Measurement of photoluminescence efficiency of Ir (III) phenylpyridine derivatives in solution and solid-state films,” Chemical Physics Letters, 460(1-3), 155-157 (2008).
[25] D. Peceli, S. Webster, D. A. Fishman *et al.*, “Optimization of the Double Pump–Probe Technique: Decoupling the Triplet Yield and Cross Section,” The Journal of Physical Chemistry A, 116(20), 4833-4841 (2012).
[26] S. Tofighi, P. Zhao, R. M. O’Donnell *et al.*, “Fast Triplet Population in Iridium (III) Complexes with Less than Unity Singlet to Triplet Quantum Yield,” The Journal of Physical Chemistry C, 123(22), 13846-13855 (2019).
[27] S. Tofighi, P. Zhao, R. M. O'Donnell *et al.*, "Quantum Yield Measurement of Organometallic Complexes using Double Pump Probe Technique." 1-4.
[28] S. Tofighi, M. V. Bondar, R. M. O’Donnell *et al.*, "Ultra-fast relaxation and singlet-triplet conversion quantum yield of Ir complexes." JTu3A. 7.
[29] M. Sheik-Bahae, A. A. Said, T.-H. Wei *et al.*, “Sensitive measurement of optical nonlinearities using a single beam,” IEEE journal of quantum electronics, 26(4), 760-769 (1990).

[30] M. R. Ferdinandus, H. Hu, M. Reichert *et al.*, “Beam deflection measurement of time and polarization resolved ultrafast nonlinear refraction,” Optics Letters, 38(18), 3518-3521 (2013).
[31] M. Sheik-Bahae, A. A. Said, and E. W. Van Stryland, “High-sensitivity, single-beam n 2 measurements,” Optics letters, 14(17), 955-957 (1989).
[32] M. Sheik-Bahae, J. Wang, R. DeSalvo *et al.*, “Measurement of nondegenerate nonlinearities using a two-color Z scan,” Optics letters, 17(4), 258-260 (1992).
[33] T. Xia, D. Hagan, M. Sheik-Bahae *et al.*, “Eclipsing Z-scan measurement of λ/10 4 wave-front distortion,” Optics letters, 19(5), 317-319 (1994).
[34] M. Sheik-Bahae, A. A. Said, D. J. Hagan *et al.*, “Nonlinear refraction and optical limiting in,” Optical engineering, 30(8), 1228-1236 (1991).
[35] T. R. Ensley, S. Benis, H. Hu *et al.*, “Nonlinear refraction and absorption measurements of thin films by the dual-arm Z-scan method,” Applied optics, 58(13), D28-D33 (2019).
[36] M. R. Ferdinandus, M. Reichert, T. R. Ensley *et al.*, “Dual-arm Z-scan technique to extract dilute solute nonlinearities from solution measurements,” Optical Materials Express, 2(12), 1776-1790 (2012).
[37] H.-J. Chang, M. V. Bondar, T. Liu *et al.*, “Electronic Nature of Neutral and Charged Two-Photon Absorbing Squaraines for Fluorescence Bioimaging Application,” ACS omega, 4(12), 14669-14679 (2019).
[38] R. A. Negres, J. M. Hales, A. Kobyakov *et al.*, “Experiment and analysis of two-photon absorption spectroscopy using a white-light continuum probe,” IEEE journal of quantum electronics, 38(9), 1205-1216 (2002).
[39] S. N. Swatton, K. R. Welford, R. C. Hollins *et al.*, “A time resolved double pump–probe experimental technique to characterize excited-state parameters of organic dyes,” Applied physics letters, 71(1), 10-12 (1997).
[40] M. Cho, S. J. Rosenthal, N. F. Scherer *et al.*, “Ultrafast solvent dynamics: Connection between time resolved fluorescence and optical Kerr measurements,” The Journal of chemical physics, 96(7), 5033-5038 (1992).
[41] M. Reichert, H. Hu, M. R. Ferdinandus *et al.*, “Temporal, spectral, and polarization dependence of the nonlinear optical response of carbon disulfide,” Optica, 1(6), 436-445 (2014).
[42] M. Reichert, H. Hu, M. R. Ferdinandus *et al.*, “Temporal, spectral, and polarization dependence of the nonlinear optical response of carbon disulfide: erratum,” Optica, 3(6), 657-658 (2016).
[43] P. Zhao, M. Reichert, S. Benis *et al.*, “Temporal and polarization dependence of the nonlinear optical response of solvents,” Optica, 5(5), 583-594 (2018).
[44] S. Benis, D. J. Hagan, and E. W. Van Stryland, "Enhancement mechanism of nonlinear optical response of transparent conductive oxides at epsilon-near-zero." 1-2.
[45] P. Zhao, M. Reichert, D. J. Hagan *et al.*, “Dispersion of nondegenerate nonlinear refraction in semiconductors,” Optics express, 24(22), 24907-24920 (2016).
[46] J. M. Hales, S.-H. Chi, T. Allen *et al.*, "Third-order nonlinear optical coefficients of Si and GaAs in the near-infrared spectral region." JTu2A. 59.
[47] S. Benis, D. J. Hagan, and E. W. Van Stryland, "Cross-propagating beam-deflection measurements of third-order nonlinear optical susceptibility." 10088, 100880N.
[48] M. Reichert, P. Zhao, J. M. Reed *et al.*, “Beam deflection measurement of bound-electronic and rotational nonlinear refraction in molecular gases,” Optics Express, 23(17), 22224-22237 (2015).
[49] M. Reichert, P. Zhao, J. M. Reed *et al.*, “Beam deflection measurement of bound-electronic and rotational nonlinear refraction in molecular gases: erratum,” Optics express, 24(17), 19122-19122 (2016).
[50] C. Karras, M. Chemnitz, R. Heintzmann *et al.*, “Impact of deuteration on the ultrafast nonlinear optical response of toluene and nitrobenzene,” Optics express, 27(21), 29491-29500 (2019).

[51] K. Schaarschmidt, M. Chemnitz, R. Scheibinger *et al.*, "Third Harmonic Generation with Ultrashort Pulses in a C2Cl4 filled Liquid Core Fiber." cd_12_3.
[52] M. Eftekhar, Z. Sanjabi-Eznaveh, H. Lopez-Aviles *et al.*, "Accelerated nonlinear interactions in graded-index multimode fibers," Nature communications, 10(1), 1-10 (2019).
[53] K. Schaarschmidt, H. Xuan, J. Kobelke *et al.*, "Long-term stable supercontinuum generation and watt-level transmission in liquid-core optical fibers," Optics letters, 44(9), 2236-2239 (2019).
[54] R. Eisenberg, and H. B. Gray, "Noninnocence in metal complexes: A dithiolene dawn," Inorganic chemistry, 50(20), 9741-9751 (2011).
[55] P. Zhao, S. Tofighi, R. M. O'Donnell *et al.*, "Electronic nature of new Ir (III) complexes: linear spectroscopic and nonlinear optical properties," The Journal of Physical Chemistry C, 121(42), 23609-23617 (2017).
[56] N. Thantu, and R. S. Schley, "Ultrafast third-order nonlinear optical spectroscopy of chlorinated hydrocarbons," Vibrational spectroscopy, 32(2), 215-223 (2003).